# Multiple-excitation pathways in a four-charged-particle system: A Green-function analysis

J. Berakdar*
*Max-Planck-Institut für Mikrostrukturphysik, Weinberg 2, 06120 Halle, Germany*
(Received 27 June 2000; published 7 December 2000)

When a charged particle interacts with an atom it may induce double electronic transitions. The complete information on such a reaction is encompassed in the Green function of the interacting four-particle system (the external charged particle, the two electrons, and the residual ion). In this work we employ a perturbation expansion of the Green operator and derive from that a multiple-scattering series for the scattering operator. As pointed out here, each term in this series corresponds to a particular sequence of binary potential collisions. From a simple analytical analysis we identify the regions of the four-body spectrum where the effects of the multiple-scattering terms become prevalent. We uncover the existence of a left-right asymmetry in a two-particle collision. This dichroic feature occurs because the symmetry of space is broken by the presence of the particles not participating in the two-body encounter. We study the ionization-ionization–transfer reaction when the external charged particle is heavy. The present formal, exact analysis predicts, in addition to the Thomas peaks, a triple-star peak structure in the spectrum when considered as a function of the momenta of the ionized electron, the residual ion and the scattered projectile. It is shown that the star is two dimensional and that its shape is dependent on the velocity of the continuum electron. In addition we consider the ionization and positronium formation following the scattering of a positron from an atom. We point out that certain terms in the multiple-scattering series coincide due to the equal masses of the electron and the positron which open the way for interference effects.

DOI: 10.1103/PhysRevA.63.012706 PACS number(s): 34.80.Ht, 34.70.+e, 34.50.Fa, 34.80.Dp

## I. INTRODUCTION

Recently, there has been impressive progress in the experimental probe of the multiple, highly excited spectrum of four-body Coloumb systems [1–9]. The excited states are achieved, e.g., upon two-electron transitions in an atomic system induced by charged-particle impact. The theory for the treatment of the four-body excited spectrum is still in the development stage. The difficulties encountered here are prototypical for the theoretical treatment of many-body correlated systems: (a) With an increasing number of interacting particles (and hence of degrees of freedom) a direct numerical evaluation of the four-body Green function, which encompasses the entire spectrum of the system, becomes intractable. (b) Due to the nonintegrable character of interacting many-particle systems, an analytical approach can only be approximate. For example, one approximation employed frequently consists of neglecting the coupling of one (or more) of the four particles to the rest of the system (e.g., as done in Refs. [10–12]). This procedure thus reduces the solution of the four-particle problem to that of an interacting three-particle problem and is usually referred to as the first Born approximation (FBA). The use of the FBA model is justified by restricting the treatment to a suitable regime of the spectrum where the interaction of the decoupled particle with the rest of the system is hoped to be weak (as compared to the other interactions involved). For instance, if the four-body state is produced as the final outcome of the electron-impact double ionization of an atom [3,4,6], one tunes the experimental setup to a high velocity of the projectile electron and a small momentum transfer to the atom. The interaction of the projectile electron with the two excited electrons and the positive residual ion is then neglected. Currently, some research [13–16] is devoted to the numerically cumbersome task of treating higher-order terms in the Born series.

In view of this situation it seems useful to dismiss a numerical evaluation of the spectrum and to identify and analyze formally the structure of the possible mechanisms of excitation that are compatible with the energy and momentum conservation laws. To do that in a general and systematic way we employ a multiple-scattering expansion of the four-body scattering operator. This expansion is obtained by expressing the scattering operator in terms of the Green operator and then iterating the Lippmann-Schwinger integral equation for the four-particle Green operator.

Each term of the multiple-scattering expansion has a well-defined physical meaning. For the lowest-order terms we give a pictorial interpretation and point out where these terms are expected to contribute prominently to the spectrum. The scope is to provide a helpful guide for exploring the structure of the multidimensional spectrum and for relating the experimental observations with physical excitation mechanisms. This present approach is, however, not supposed to give (or capable of giving) a numerical estimate of each of the multiple-scattering events. In fact, the present investigation covers a wide range of processes (ion-atom collisions, electron-atom collisions, positron-atom scattering, and positronium formations,...). This is possible since we are analyzing in a formal way the many-body Green function (the resolvent of the total Hamiltonian). It should be stressed, however, that a practical (numerical) evaluation of the many-body spectrum (e.g., the trace of the imaginary part of the Green function) requires extensive approximations which are usually valid only for a specific system under study (i.e.,

*FAX: +49 345 5533221. Email address: jber@mpi-halle.de

 

reasonable approximations for ion-atom collisions might not be applicable for electron-atom scattering processes).

The plan of the paper is as follows.

In Sec. II we introduce the formal theory and derive the multiple-scattering expansion of the scattering operator. For three-particle scattering systems, the role of successive binary encounters and their manifestation in the cross section are well established [17–28]. In contrast, for the present case of four particles [1,13,27,21,14,16,11] the various multiple binary collisions are much less studied. Therefore, we consider in Sec. III the complete fragmentation channel as achieved upon double ionization by charged-particle impact. The various terms in the scattering operator expansion are then associated with multiple sequential binary encounters between the constituents of the systems. Each of the multiple-scattering events is expected to be observable as a peak in the multiparticle spectrum. To determine roughly the conditions, i.e., the angular and energy range, under which these peaks occur, we utilize the energy and momentum conservation laws and assume the particles' motion upon each binary scattering event to be uniform. It should be stressed, however, that this determination of the peak positions can be considered reasonable only when the involved particles are fast as compared to the velocity components initially contained in the system (the atom prior to the double electron transition).

The present (nonrelativistic) analysis of four-particle collision systems indicates the occurrence of a left-right asymmetry in the (binary) two-particle collision even in the absence of spin-orbit interactions. As argued in the text this effect is brought out by the break of isotropy of space due to the presence of particles other than the two colliding from each other. This effect does not appear in a three-body system because the vector momenta of two particles (say the two particles participating in a binary encounter) fix the vector momentum of the third one (via momentum conservation law). Therefore, the space, where the three-particle cross section is defined, is spanned by two vectors only. This is in contrast to the situation of four particles where the momentum conservation implies that the four-particle momentum space is dependent on *three* vectors.

In Sec. IV we analyze the multiple-scattering operator in the ionization-transfer–ionization channel, i.e., when upon a scattering of a charged particle from an atom one (atomic) electron is captured by the Coulomb field of the projectile and a second electron is ejected from the target atom. Here we discuss two distinct situations: (a) For a heavy projectile we consider the spectrum as function of the vector momenta of the residual ion $\mathbf{k}_{\rm ion}$, the ionized electron $\mathbf{k}_2$, and of the scattered projectile $\mathbf{k}_p$. Our analysis anticipates, in addition to the Thomas peaks, a triple-star structure in the spectrum (formed by the three vectors $\hat{\mathbf{k}}_{\rm ion},\hat{\mathbf{k}}_2,\hat{\mathbf{k}}_p$). The star is two dimensional. Its shape depends on the velocity of the ionized electron. As explained in full detail in the text the star form structure is the result of a sequence of binary encounters combined with a recoil mechanism of the ionized electron from ionic core. The latter scattering can be mediated by initial state binding. We also investigate how the left-right asymmetry in the two-particle collision is being reflected in the transformational properties of the starlike structure.

(b) In the final section we consider the situation where a positron impinging on an atom results in positronium formation accompanied by the ionization of the atom. This case is of particular interest as the masses of the electrons and the positron are equal. This imposes a special constraint on the kinematical configurations for the two-particle collision. We point out that in this case some of the multiple-scattering terms appear at the same kinematical conditions and hence are indistinguishable experimentally. Therefore interference effects can be expected. Section V concludes this work with some general remarks on the merit and limitations of the present findings.

Unless otherwise stated, atomic units are used throughout.

## II. FORMAL DEVELOPMENT

To unravel the pathways leading to particle-impact double-electron transitions of an atomic system we consider an isolated atom in a (at least two-electron) state $|\varphi_a\rangle$ with an energy $\epsilon_a$. In what follows we study the double ionization of $|\varphi_a\rangle$. Similar considerations, however, apply to double excitations to states below the double ionization threshold.

Upon an external perturbation of the state $|\varphi_a\rangle$ by a monoenergetic charged particle beam (with a momentum $\mathbf{k}_0$) two electrons (hereafter referred to as the active electrons) are transferred into the double continuum and recede from the ionic core with momenta $\mathbf{k}_1$ and $\mathbf{k}_2$. The projectile emerges in the final state with a momentum $\mathbf{k}_p$. The residual ion is left in the state $|\varphi_c\rangle$ (with a binding energy $\epsilon_c$). The corresponding experiment is supposed to determine simultaneously $\epsilon_a$, $\mathbf{k}_0$ and $\epsilon_c$ $\mathbf{k}_p$, $\mathbf{k}_1$, $\mathbf{k}_2$ under the constraint of the momentum and energy conservation laws

$$\mathbf{k}_0=\mathbf{k}_p+\mathbf{k}_1+\mathbf{k}_2+\mathbf{k}_{\rm ion}, \tag{1}$$

$$E_i=E_0+\epsilon_a=E_p+E_1+E_2+E_{\rm ion}+\epsilon_c=E_f. \tag{2}$$

In these relations we refer to the momentum of the ion by $\mathbf{k}_{\rm ion}$ and to its kinetic (translational) energy by $E_{\rm ion}$. The initial and final state energies of the whole systems are $E_i$ and $E_f$ and those of the projectile are $E_0$ and $E_p$. The energies of the two emitted electrons are labeled by $E_1$ and $E_2$.

The total Hamiltonians in the *asymptotic* initial- and the final-state channels are, respectively, given by

$$H_i=h_a+h_p, \tag{3}$$

$$H_f=h_c+h_{ex}. \tag{4}$$

The operators $h_a$ and $h_c$ are the Hamiltonians of the undisturbed atom in the initial state and that of the residual ion, i.e., $h_a|\varphi_a\rangle=\epsilon_a|\varphi_a\rangle$ and $h_c|\varphi_c\rangle=\epsilon_c|\varphi_c\rangle$.

The Hamiltonian of the impinging projectile is $h_p$. Furthermore, $h_{ex}$ is the Hamiltonian of final-state continuum fragments in the asymptotic region (for large interparticle separation). In this study we skip the discussion of the effects of the infinite range of the Coloumb potentials and assume hereafter that all potentials are of finite range so that standard

methods of scattering theories (Lippmann-Schwinger equations, asymptotic free particle states, etc.) are applicable.

Denoting the total Hamiltonian of the system by $H$ we can thus define final ($V_f$) and initial-state ($V_i$) transition potential operates as

$$V_f = H - H_{\rm f} = V_{pe_1} + V_{pe_2} + V_{e_1e_2} + V_{e_1{\rm c}} + V_{e_2{\rm c}} + V_{p{\rm c}}, \tag{5}$$

$$V_i = H - H_i = V_{pe_1} + V_{pe_2} + V_{p{\rm c}}. \tag{6}$$

Here $V_{pe_{1/2}}$ is the two-particle Coulomb interactions between the projectile and the *active* electrons, $V_{p{\rm c}}$ is the interaction potential between the projectile and the final-state ionic core, and $V_{e_{1/2}{\rm c}}$ is the scattering potential of the ionized electrons from the ionic core. Moreover, $V_{e_1e_2}$ is the Coulomb interaction between the active electrons.

The Hamiltonians $H_i$ and $H_f$ describe the same projectile-atom system, however with different boundary conditions (a neutral ground state atom and an undistorted projectile in case of $H_i$ and three-charged continuum particles in the field of a doubly charged ion in case of $H_f$). Therefore the relation applies

$$h_a = h_c + V_{e_1c} + V_{e_2c} + V_{e_1e_2}. \tag{7}$$

The probability for the system to go over from the state $|\mathbf{k}_0, \varphi_a\rangle$ (where $H_i|\mathbf{k}_0, \varphi_a\rangle = E_i|\mathbf{k}_0, \varphi_a\rangle$) into the excited state $|\mathbf{k}_p, \mathbf{k}_1, \mathbf{k}_2, \varphi_{\rm c}\rangle$ (where $H_f|\mathbf{k}_p, \mathbf{k}_1, \mathbf{k}_2, \varphi_{\rm c}\rangle = E_f|\mathbf{k}_p, \mathbf{k}_1, \mathbf{k}_2, \varphi_{\rm c}\rangle$) is determined by the scattering matrix element $\sigma(\mathbf{k}_p, \mathbf{k}_1, \mathbf{k}_2, \varphi_{\rm c}; \mathbf{k}_0, \varphi_a)$ where

$$\begin{aligned}\sigma(\mathbf{k}_p, \mathbf{k}_1, \mathbf{k}_2, \varphi_{\rm c}; \mathbf{k}_0, \varphi_a) &= \langle \mathbf{k}_0, \varphi_a | S | \mathbf{k}_p, \mathbf{k}_1, \mathbf{k}_2, \varphi_{\rm c}\rangle \\ &= \langle \Psi^- | \Psi^+ \rangle. \end{aligned} \tag{8}$$

The experimentally interesting part of these matrix elements satisfies the constraints (1) and (2). The state vectors $|\Psi^\pm\rangle$ are related to the asymptotic (detector) states via

$$|\Psi^-\rangle = \Omega_f^- |\mathbf{k}_p, \mathbf{k}_1, \mathbf{k}_2, \varphi_{\rm c}\rangle, \tag{9}$$

$$|\Psi^+\rangle = \Omega_i^+ |\mathbf{k}_0, \varphi_a\rangle. \tag{10}$$

The wave operators $\Omega_f^-, \Omega_i^+$ are given by

$$\Omega_f^- = \mathbf{1} + G^- V_f, \tag{11}$$

$$\Omega_i^+ = \mathbf{1} + G^+ V_i. \tag{12}$$

The many-body Green operator $G^\pm$ is the resolvent of $H$ with appropriate boundary conditions. From Eqs. (5) and (6) we deduce the integral equations

$$G^- = G_f^- + G_f^- V_f G^-, \tag{13}$$

$$G^+ = G_i^+ + G_i^+ V_i G^+, \tag{14}$$

where $G_f^-$ and $G_i^+$ are the resolvents of $H_f$ and $H_i$ [Eqs. (4) and (3)], with the appropriate boundary conditions.

As stated above the Hamiltonians $h_a$ and $h_p$ in Eq. (3), as well as $h_c$ and $h_{ex}$ in Eq. (4), are decoupled (as a matter of definition). Therefore, the following relations apply:

$$G_f^- = g_{\rm c}^- g_{\rm ex}^- =: G_c^-, \tag{15}$$

$$G_i^+ = g_a^+ g_p^+ =: G_a^+. \tag{16}$$

The Green operators of the atom and the residual ionic core are denoted by $g_a^+$ and $g_{\rm c}^-$, respectively. $g_p^+$ and $g_{\rm ex}^-$ are the resolvents of $h_p$ and $h_{\rm ex}$.

Furthermore, a relation between $g_a^+$ and $g_{\rm c}^+$ can be established by means of Eq. (7),

$$g_a^+ = g_c^+ + g_c^+ (V_{e_1c} + V_{e_2c} + V_{e_1e_2}) g_a^+. \tag{17}$$

From Eqs. (8)–(10) we can write $\sigma = \langle \mathbf{k}_p, \mathbf{k}_{e_1}, \mathbf{k}_{e_2}, \varphi_{\rm c} | \Omega_f^{-\dagger} \Omega_i^+ | \mathbf{k}_0, \varphi_a\rangle$. Therefore, all dynamical quantities are contained in the product of the two wave operators (this product is usually called the scattering $S$ operator).

For completeness we note that the $S$-matrix elements can be expressed in terms of the transition-matrix elements $\mathcal{T}_{if}$ (from which cross sections are readily obtained). In the post form this interrelation is given by

$$\begin{aligned}&\langle \mathbf{k}_p, \mathbf{k}_{e_1}, \mathbf{k}_{e_2}, \varphi_{\rm c} | S | \mathbf{k}_0, \varphi_a\rangle \\ &\quad = \langle \mathbf{k}_p, \mathbf{k}_{e_1}, \mathbf{k}_{e_2}, \varphi_{\rm c} | \mathbf{k}_0, \varphi_a\rangle - 2i\pi\, \delta(E_f - E_i) \\ &\qquad \times \langle \mathbf{k}_p, \mathbf{k}_{e_1}, \mathbf{k}_{e_2}, \varphi_{\rm c} | V_f | \Psi^+\rangle, \end{aligned} \tag{18}$$

whereas in the prior form the following equation applies:

$$\begin{aligned}&\langle \mathbf{k}_p, \mathbf{k}_{e_1}, \mathbf{k}_{e_2}, \varphi_{\rm c} | S | \mathbf{k}_0, \varphi_a\rangle \\ &\quad = \langle \mathbf{k}_p, \mathbf{k}_{e_1}, \mathbf{k}_{e_2}, \varphi_{\rm c} | \mathbf{k}_0, \varphi_a\rangle - 2i\pi\, \delta(E_f - E_i) \\ &\qquad \times \langle \Psi^- | V_i | \mathbf{k}_0, \varphi_a\rangle. \end{aligned} \tag{19}$$

The transition-matrix elements are

$$\mathcal{T}_{fi} := \langle \mathbf{k}_p, \mathbf{k}_{e_1}, \mathbf{k}_{e_2}, \varphi_{\rm c} | V_f | \Psi^+\rangle = \langle \Psi^- | V_i | \mathbf{k}_0, \varphi_a\rangle =: \mathcal{T}_{if}. \tag{20}$$

Hence the prime quantity that encompasses the collision dynamics is

$$\begin{aligned}\Omega_f^{-\dagger} \Omega_i^+ &= (\mathbf{1} + V_f G^{-\dagger})(\mathbf{1} + G^+ V_i) \\ &= \mathbf{1} + G^+ V_i + V_f G^{-\dagger} + V_f G_f^{-\dagger} G^+ V_i \end{aligned} \tag{21}$$

$$= \mathbf{1} + A + B + C, \tag{22}$$

where the leading-order terms of $A$, $B$, and $C$ are

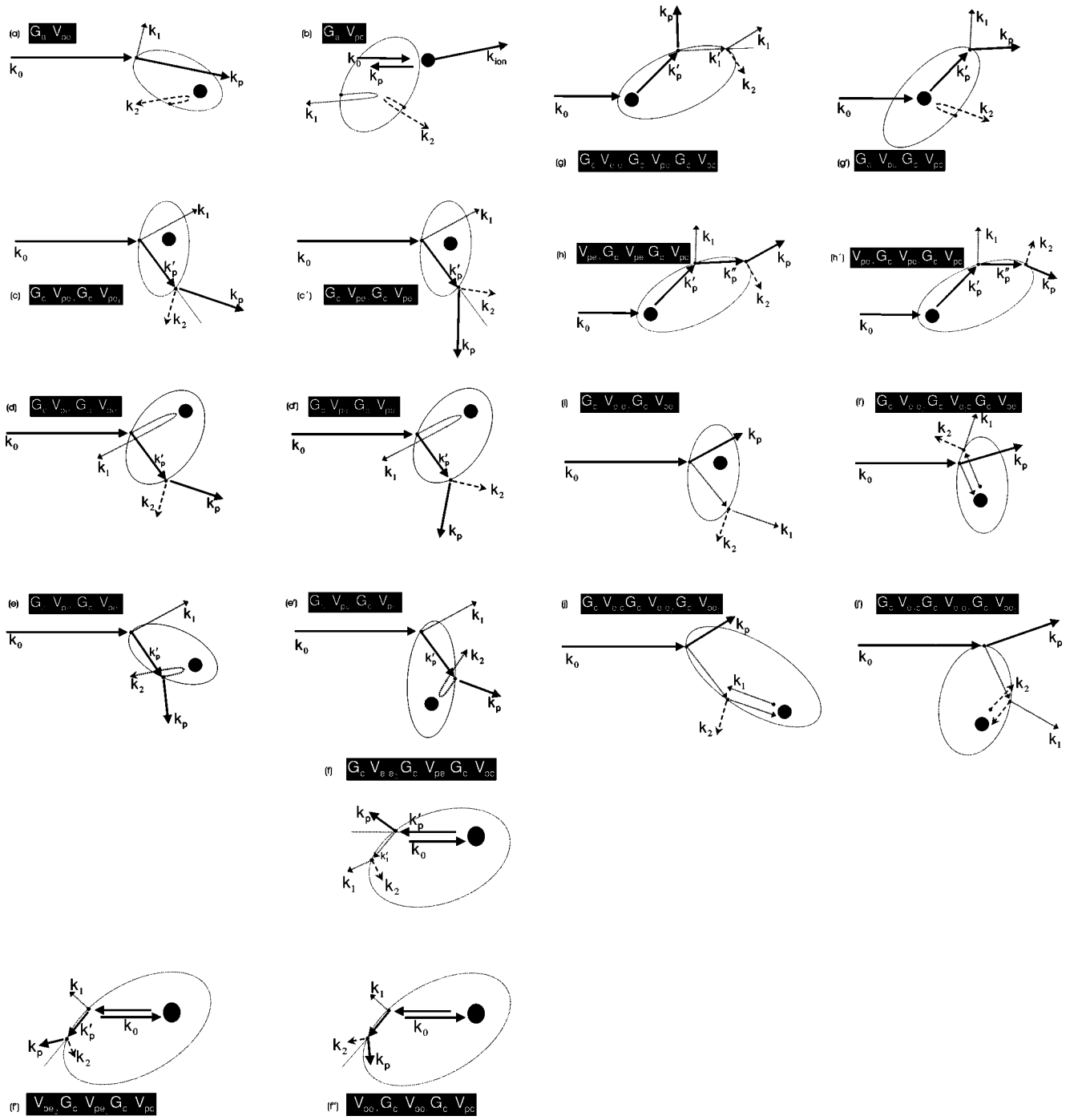

FIG. 1. Double-electron transitions induced by charged-particle impact. The schematic drawings show multiple-scattering processes that correspond to some of the terms in the expansion (23)–(32) (see text for details). The respective terms are shown in each set. The momenta of the two excited electrons are referred to by $\mathbf{k}_1$ and $\mathbf{k}_2$ whereas the momenta of the incoming and the scattered projectile are labeled, respectively, by $\mathbf{k}_0$ and $\mathbf{k}_p$.

$$
\begin{aligned}
A = {} & G_a^+ V_{pe_1} + G_a^+ V_{pe_2} + G_a^+ V_{pc} + G_a^+ V_{pe_1} G_a^+ V_{pe_2} \\
& + G_a^+ V_{pe_1} G_a^+ V_{pc} + G_a^+ V_{pe_2} G_a^+ V_{pe_1} \\
& + G_a^+ V_{pe_2} G_a^+ V_{pc} + G_a^+ V_{pc} G_a^+ V_{pe_1} \\
& + G_a^+ V_{pc} G_a^+ V_{pe_2} + G_a^+ V_{pe_2} G_a^+ V_{pe_1} G_a^+ V_{pc} \\
& + G_a^+ V_{pe_2} G_a^+ V_{pc} G_a^+ V_{pe_1} + G_a^+ V_{pc} G_a^+ V_{pe_1} G_a^+ V_{pe_2} \\
& + G_a^+ V_{pc} G_a^+ V_{pe_2} G_a^+ V_{pe_1} + \cdots , \qquad (23)
\end{aligned}
$$

$$
B = \sum_{j=1}^{7} B_j , \qquad (24)
$$

$$B_1 = V_{pe_1}G_c^+ + V_{pe_2}G_c^+ + V_{e_1c}G_c^+ + V_{pc}G_c^+ + V_{e_1e_2}G_c^+ + V_{e_2c}G_c^+ + V_{pe_1}G_c^+V_{pe_1}G_c^+ + V_{pe_2}G_c^+V_{pe_2}G_c^+ + V_{e_1e_2}G_c^+V_{e_1e_2}G_c^+ + \cdots, \quad (25)$$

$$B_2 = V_{pe_1}G_c^+V_{pc}G_c^+ + V_{pe_1}G_c^+V_{e_1c}G_c^+ + V_{pe_1}G_c^+V_{pe_2}G_c^+ + V_{pe_1}G_c^+V_{e_1e_2}G_c^+ + V_{pe_1}G_c^+V_{e_2c}G_c^+, \quad (26)$$

$$B_3 = V_{pc}G_c^+V_{pe_1}G_c^+ + V_{pc}G_c^+V_{e_1c}G_c^+ + V_{pc}G_c^+V_{pe_2}G_c^+ + V_{pc}G_c^+V_{e_1e_2}G_c^+ + V_{pc}G_c^+V_{e_2c}G_c^+, \quad (27)$$

$$B_4 = V_{e_1c}G_c^+V_{pe_1}G_c^+ + V_{e_1c}G_c^+V_{pc}G_c^+ + V_{e_1c}G_c^+V_{pe_2}G_c^+ + V_{e_1c}G_c^+V_{e_1e_2}G_c^+ + V_{e_1c}G_c^+V_{e_2c}G_c^+, \quad (28)$$

$$B_5 = V_{pe_2}G_c^+V_{pe_1}G_c^+ + V_{pe_2}G_c^+V_{pc}G_c^+ + V_{pe_2}G_c^+V_{e_1c}G_c^+ + V_{pe_2}G_c^+V_{e_1e_2}G_c^+ + V_{pe_2}G_c^+V_{e_2c}G_c^+, \quad (29)$$

$$B_6 = V_{e_1e_2}G_c^+V_{pe_1}G_c^+ + V_{e_1e_2}G_c^+V_{pc}G_c^+ + V_{e_1e_2}G_c^+V_{e_1c}G_c^+ + V_{e_1e_2}G_c^+V_{pe_2}G_c^+ + V_{e_1e_2}G_c^+V_{e_2c}G_c^+, \quad (30)$$

$$B_7 = V_{e_2c}G_c^+V_{pe_1}G_c^+ + V_{e_2c}G_c^+V_{pc}G_c^+ + V_{e_2c}G_c^+V_{e_1c}G_c^+ + V_{e_2c}G_c^+V_{pe_2}G_c^+ + V_{e_2c}G_c^+V_{e_1e_2}G_c^+, \quad (31)$$

$$\begin{aligned} C = {} & V_{pe_1}G_c^+G_a^+V_{pe_1} + V_{pe_1}G_c^+G_a^+V_{pe_2} \\ & + V_{pe_1}G_c^+G_a^+V_{pc} + V_{pe_2}G_c^+G_a^+V_{pe_1} \\ & + V_{pe_2}G_c^+G_a^+V_{pe_2} + V_{pe_2}G_c^+G_a^+V_{pc} + V_{pc}G_c^+G_a^+V_{pe_1} \\ & + V_{pc}G_c^+G_a^+V_{pe_2} + V_{pc}G_c^+G_a^+V_{pc} + V_{e_1e_2}G_c^+G_a^+V_{pe_1} \\ & + V_{e_1e_2}G_c^+G_a^+V_{pe_2} + V_{e_1e_2}G_c^+G_a^+V_{pc} + V_{e_1c}G_c^+G_a^+V_{pe_1} \\ & + V_{e_1c}G_c^+G_a^+V_{pe_2} + V_{e_1c}G_c^+G_a^+V_{pc} + V_{e_2c}G_c^+G_a^+V_{pe_1} \\ & + V_{e_2c}G_c^+G_a^+V_{pe_2} + V_{e_2c}G_c^+G_a^+V_{pc} + \cdots. \end{aligned} \quad (32)$$

Equations (23)–(32) are readily derived by iterating the integral (Lippmann-Schwinger) equations (13) and (14) and considering the lowest terms. Higher-order terms are just a multiple iteration of each of the components of Eqs. (23) and (32).

### III. DOUBLE-IONIZATION PATHWAYS

The multiple-scattering expansions (23)–(32) offer a direct insight into the ionization paths as visualized in Figs. 1(a)–1(j′). In general, the continuum spectrum is determined by a coherent sum of all the terms (23)–(32). Thus, interferences between the amplitudes of these terms may take place, as discussed in this paper in case of positronium formation. However, in some regions of the spectrum (which can be selectively probed by an appropriate experiment) some of the terms in Eqs. (23)–(32) are particularly dominant. It is our purpose here to single out these regions and to determine the (rough) positions in the spectrum where the effect of the individual terms in Eqs. (23)–(32) becomes apparent. It should be noted from the outset that this determination procedure assumes high impact and high excess energies, i.e., $E_0 \gg \epsilon_a$ and $(E_p + E_1 + E_2) \gg \epsilon_c$.

The interpretation of the individual terms of Eqs. (23)–(32) is as follows.

(1) The unity operator in Eq. (22) corresponds to the nonscattered part.

(2) The first (or second) term in Eq. (23) describes an electron-projectile encounter in the field of the atom [Fig. 1(a)]. The second electron (not interacting directly with the projectile) is emitted by means of scattering from the ionic core and the first electron. This scattering is encompassed in $G_a$ [cf. Eq. (17)], i.e., in the undisturbed target system. The kinematical conditions for this process are as follows: $\mathbf{k}_1 \approx \mathbf{k}_0 - \mathbf{k}_p$ and $\mathbf{k}_{\rm ion} \approx -\mathbf{k}_2$. The assumption underlying this picture is $E_1 \approx E_0 - \epsilon_a$ and $E_2 < \epsilon_a$.

(3) The second term in Eq. (23) can be interpreted [see Fig. 1(b)] as a direct scattering of the projectile from the ionic core (the atom except for the active electrons). The two active electrons are then ejected due to electron-electron scattering (and electron-core scattering) as contained in $G_a$ [cf. Eq. (17)]. The kinematical conditions for this process are $\mathbf{k}_p \approx -\mathbf{k}_0$, $\mathbf{k}_{\rm ion} \approx 2\mathbf{k}_0$, and $\mathbf{k_1} \approx -\mathbf{k}_2$. Here it is assumed that the experimental conditions are such that $E_1 \approx E_2 < \epsilon_a$ and the velocity of the incoming projectile is much higher than that of the ejected electrons.

(4) The fourth and sixth terms of the expansion (23) are schematically shown in Fig. 1(c): after a binary collision of the projectile with one of the active electrons, it scatters from the second active electron. This sequential process shows up in the spectrum at [cf. Fig. 1(c)]: $\mathbf{k}_1 \approx \mathbf{k}_0 - \mathbf{k}_p'$, $\mathbf{k}_{\rm ion} \approx 0$ and $\mathbf{k}_2 \approx \mathbf{k}_p' - \mathbf{k}_p$. If the projectile possesses the same mass $m_p$ as the electron mass $m_e$ we arrive at $\mathbf{k}_2 \perp \mathbf{k}_p$, $k_2^2 + k_p^2 = k_p'^2$ and $\mathbf{k}_1 \perp \mathbf{k}_p'$, $k_1^2 + k_p'^2 = k_0^2$. For this process we assume that $E_1$ and $E_2$ (and $E_0$) are much larger than $\epsilon_a$.

It is important to note here that due to the presence of *two* electrons in the continuum (in addition to the scattered projectile) an intermediate two-particle collision shows a left-right asymmetry. This dichroic effect is illustrated in Figs. 1(c) and 1(c′): The whole experiment as shown in Figs. 1(c) and 1(c′) is cylindrically symmetric with respect to $\mathbf{k}_0$. However, the two-particle collision between the scattered projectile with (intermediate) momentum $\mathbf{k}_p'$ and the second electron (escaping with momentum $\mathbf{k}_2$) is generally *not* cylindrically symmetric with respect to $\mathbf{k}_p'$. I.e., in general the processes depicted in Figs. 1(c) and 1(c′) are not identical and will have different matrix elements. This dichroic effect is correlation induced. It is strongly dependent on the interaction of the first electron (with momentum $\mathbf{k}_1$) with the

projectile and the second electron. In other words if electron ''1'' does not interact with the second electron and with the scattered projectile in the final state, it would not see the difference between the diagrams shown in Figs. 1(c) and1 (c′). The auxiliary momentum $\mathbf{k}_p'$ cannot be detected in the experiment; it can, however, be deduced from Fig. 1(c) once the measured spectrum can be identified with the scattering mechanism depicted in Fig. 1(c).

In a *single*-ionization experiment the first scattering event [shown in Figs. 1(c) and 1($c'$)] between the projectile and the first electron results in the well-known ''binary peak'' [29]. At the opposite direction of the binary peak a further structure appears which is called the ''recoil peak'' and originates from the scattering of the ionized electron from the ionic core [29].

In the present situation of double ionization the recoil peak can be identified by examining the terms shown pictorially in Figs. 1(d)–1(e′). In Fig. 1(d) one of the atomic electrons recoils off the nucleus after a collision with the projectile. The recoil process can in principle be facilitated by initial-state binding [i.e., by $G_a$ as given by Eq. (17)] or by the final-state interaction of this electron with the ionic core. The second electron is then ionized upon a single interaction with the projectile. This latter process is not cylindrically symmetric with respect to $\mathbf{k}_p'$. Therefore, in general there will be a difference between Figs. 1(d) and 1(d′) [and Figs. 1(e) and 1(e′)]. The kinematical conditions under which the processes Figs. 1(d) and 1(d′) are observable in the spectrum are respectively those of Fig. 1(c) and 1(c′) except for $\mathbf{k}_{\rm ion}\approx-\mathbf{k}_1$. In addition, this interpretation assumes that $E_2\gg E_1$ (and $E_0\gg\epsilon_a$).

In the cases shown in Figs. 1(e) and 1(e′) the first electron escapes directly into the continuum after a single collision with the projectile. The projectile scatters then from the second electron and this electron recoils off the ionic core. The kinematical conditions are then those discussed in Fig. 1(c′) but the ion has a finite momentum $\mathbf{k}_{\rm ion}\approx-\mathbf{k}_2$.

(6) In Figs. 1(f)–1(f″) the mechanisms for the projectile's (elastic) backreflection are displayed along with the respective transition operators [cf. Eq. (23)]. These mechanisms are particularly relevant for lighter projectiles ($m_p\ll m_c$, where $m_c$ is the mass of the ionic core). Again we notice the appearance of the dichroic effect in Figs. 1(f′) and 1(f″). In cases of Figs. 1(f)–1(f″) one expects $\mathbf{k}_{\rm ion}\approx2\mathbf{k}_0$. The emergence directions of the collision fragments can then be determined from Eqs. (1) and (2). For example, if $m_p=m_e$ we arrive for the process of Fig. 1(f) at $\mathbf{k}_1\perp\mathbf{k}_2$ and $k_1^2+k_2^2=k_1'^2$. In addition $\mathbf{k}_p\perp\mathbf{k}_1'$ and $k'^2_1+k_p^2=k_p'^2\approx k_0^2$. Hence, if $\mathbf{k}_{\rm ion}$ and $\mathbf{k}_p$ are determined one can deduce $\mathbf{k}_1'$.

The processes of Figs. 1(f,f′,f″) are distinguishable in that in Fig. 1(f) the two electrons emerge in the same half plane (with respect to $\mathbf{k}_0$) whereas in Figs. 1(f′) and 1(f″) the active electrons emerge in different half planes. In Fig. 1(f′) the projectile escapes in between the emission directions of the electrons in contrast to the case shown in Fig. 1(f″).

(7) Further scattering mechanisms in which a direct scattering of the projectile from the ionic core is involved are shown in Figs. 1(g)–1(h′). In Fig. 1(g) the projectile scatters from the ionic core and then from one of the active electrons. This excited electron collides then with the other electron and both emerge with momenta $\mathbf{k}_1$ and $\mathbf{k}_2$. The kinematical conditions associated with this process are readily derived from Eqs. (1) and (2): $\mathbf{k}_1\perp\mathbf{k}_2$ and $k_1^2+k_2^2=k_1'^2$, whereas $\mathbf{k}_p'=\mathbf{k}_0-\mathbf{k}_{\rm ion}$. If $m_p=m_e$ then we obtain the relation $\mathbf{k}_p\perp(\mathbf{k}_1+\mathbf{k}_2)$.

As indicated by the fifth term of Eq. (23) [cf. Fig. 1(g′)], a scattering process may take place in which the projectile is scattered from the ionic core. It undergoes subsequently a single collision with one of the active electrons which is then ejected. The second active electron is emitted by means of scattering from the potentials encompassed in $G_a$ [Eq. (17)].

The conditions under which the influence of the process Fig. 1(g′) may appear are $\mathbf{k}_p'\approx\mathbf{k}_1+\mathbf{k}_p$. If $m_p=m_e$ then we deduce $\mathbf{k}_1\perp\mathbf{k}_p$ and $k_p^2+k_1^2=k_p'^2\approx k_0^2$. By determining $\mathbf{k}_1$ and $\mathbf{k}_p$ the intermediate momentum $\mathbf{k}_p'$ is determined. For small $|\mathbf{k}_2|$ we arrive then at $\mathbf{k}_{\rm ion}\approx\mathbf{k}_0-\mathbf{k}_p'$. The assumption underlying this process is that $E_0\gg\epsilon_a\ll E_1\approx E_2$. We note that in case of a light projectile (with respect to the ionic core mass) the impinging projectile can scatter everywhere in space. Therefore, the momentum vectors of the continuum particles are not necessarily linearly dependent, i.e., they do not need to be in one plane.

(8) In Figs. 1(h) and 1(h′) the projectile successively scatters from both of the active electrons following an encounter with the ionic core. The difference between the processes depicted in Figs. 1(h) and 1(h′) is due to the aforementioned left-right asymmetry (with respect to $\mathbf{k}_p''$) in the scattering of the projectile from electron ''2.'' In the illustration of Figs. 1(h) and 1(h′) the processes 1(h′) and 1(h) are distinguishable, for in case of Fig. 1(h′) both electrons emerge in the same half plane (with respect to $\mathbf{k}_0$) whereas in case of Fig. 1(h) the electrons emerge in different half planes. The kinematical conditions under which the processes of Figs. 1(h) and 1(h′) show up are readily derived from Eqs. (1) and (2). Our interpretation is valid under the assumption that $E_0\gg\epsilon_a\ll E_1\approx E_2$. For light projectiles, the processes shown Figs. 1(g) and 1(h′) provide a major contribution to out-of-plane scattering.

(9) In Figs. 1(i) and 1(j′) few multiple double-scattering mechanisms are depicted in which the electron-electron scattering is involved. In all of these cases the projectile scatters once from one of the active electrons. Subsequently a scattering of this excited electron from the other active electron (and/or from the ionic core) leads to double ionization. For the process shown in Fig. 1(i) Eqs. (1) and (2) yield $\mathbf{k}_1\perp\mathbf{k}_2$ and $\mathbf{k}_{\rm ion}\approx0$. In contrast, for the case of Fig. 1(i′) we obtain the kinematical condition $\mathbf{k}_1\perp\mathbf{k}_2$, $\mathbf{k}_{\rm ion}\approx-2(\mathbf{k}_1+\mathbf{k}_2)$, and $\mathbf{k}_0+\mathbf{k}_p=-(\mathbf{k}_1+\mathbf{k}_2)$. In Fig. 1(j) we encounter the same situation as in Fig. 1(i); however, one of the electrons recoils off the ion after the electron-electron single collision. Thus the same kinematical conditions as Fig. 1(i) apply to Fig. 1(j) except that $\mathbf{k}_{\rm ion}\approx-2\mathbf{k}_1$. The process shown in Fig. 1(j′) is a result of the left-right asymmetry in the electron-electron single collision. It can be distinguished from Fig. 1(j) by an

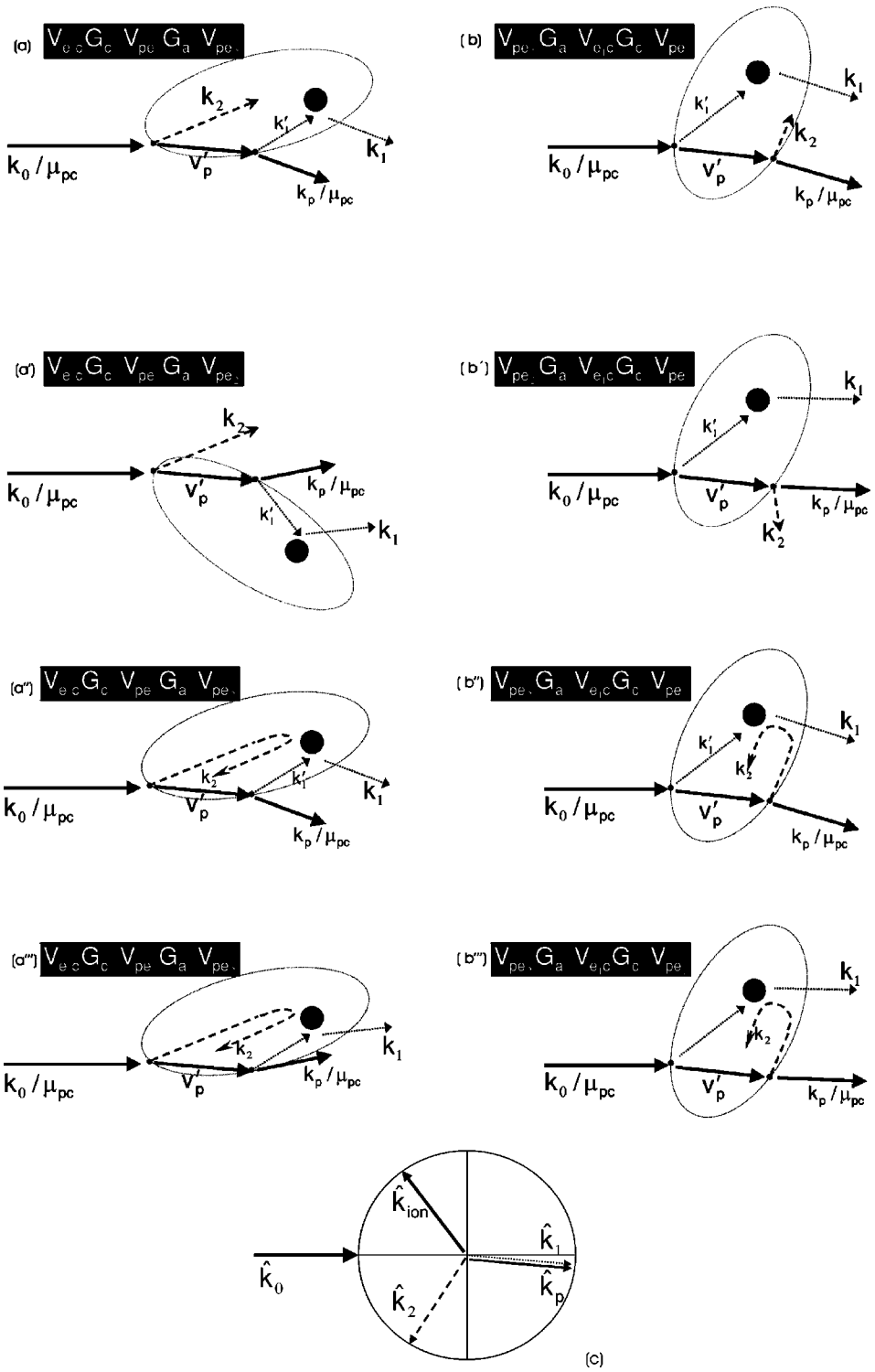


FIG. 2. A pictorial representation of the multistep scattering processes that are involved in the ionization-transfer–ionization reaction triggered by a heavy charged projectile. The momentum of the electron to be transferred to the projectile is indicated by $\mathbf{k}_1$ whereas the $\mathbf{k}_2$ stands for the momentum of the ionized electron. $\mathbf{k}_0$ and $\mathbf{k}_p$ stand for the momenta of the incoming and the scattered projectiles, respectively.

appropriate arrangement of the experiment as illustrated in Figs. 1(j) and 1(j′).

## IV. IONIZATION AND REARRANGEMENT COLLISIONS

In Fig. 1 we illustrated and discussed the mechanisms leading to double-electron escape. In this section we study ionization processes that are accompanied by a capture of one of the ionized electrons into the Coulomb field of the projectile. Figures 2(a)–2(d) give a pictorial representation of the first-order multiple-scattering terms that are relevant to the ionization-transfer–ionization channel. In what follows the electron to be captured by the projectile is assumed to be the one whose momentum is indexed by ''1.''

For the capture process to be effective electron 1 and the scattered projectile have to emerge with equal velocity vectors. In the center-of-mass system this im-

plies $\mathbf{k}_1/m_e =: \mathbf{v}_1 = \mathbf{v}_p := \mathbf{k}_p/\mu_{pc}$ (cf. Fig. 2). Here we neglected terms of the order $m_e/m_c$ and defined the projectile-ion reduced mass as $\mu_{pc} = (m_p m_c)/(m_p + m_c)$.

### A. Heavy projectile impact

In Fig. 2(a) the projectile scatters from electron ''2'' and propagates further with momentum $\mathbf{k}_p'$, velocity $\mathbf{v}_p'$, and energy $E_p'$. It scatters then from electron 1 to emerge with the final momentum $\mathbf{k}_p$. The excited electron 1, which acquires the momentum $\mathbf{k}_1'$, recoils from the ionic core and recedes with the momentum $\mathbf{k}_1$, as shown in the figure. From elementary algebraic considerations of Eqs. (1) and (2) we deduce the mutual angles between $\hat{\mathbf{k}}_2$ and $\hat{\mathbf{v}}_p'$ as well as between $\hat{\mathbf{k}}_0$ and $\hat{\mathbf{v}}_p'$ to be

$$\begin{aligned}\cos(\theta_{k_2,v_p'}) &= \hat{\mathbf{k}}_2 \cdot \hat{\mathbf{v}}_p' \\ &= \frac{1}{2\sqrt{\mu_{pc}}} \sqrt{\frac{E_2}{E_p'}} (\mu_{pc} - 1) \\ &= \frac{1}{2} \frac{v_2}{v_p'} \left(1 - \frac{1}{\mu_{pc}}\right), \end{aligned} \tag{33}$$

$$\cos(\theta_{k_0,v_p'}) = \hat{\mathbf{k}}_0 \cdot \hat{\mathbf{v}}_p' = \sqrt{1 - \frac{E_2}{E_0}} + \frac{E_2}{2\sqrt{E_0^2 - E_0 E_2}} (1 - 1/\mu_{pc}). \tag{34}$$

Obviously, the angles between $\hat{\mathbf{k}}_1'$ and $\hat{\mathbf{v}}_p \equiv \hat{\mathbf{k}}_p$ as well as between $\hat{\mathbf{v}}_p'$ and $\hat{\mathbf{v}}_p$ are (please note $k_1 = k_1'$)

$$\begin{aligned}\cos(\theta_{k_1',v_p}) &= \hat{\mathbf{k}}_1' \cdot \hat{\mathbf{v}}_p \\ &= \frac{1}{2} \sqrt{\frac{\mu_{pc} E_1}{E_p}} \left(1 - \frac{1}{\mu_{pc}}\right) \\ &= \frac{1}{2} \frac{v_1}{v_p} \left(1 - \frac{1}{\mu_{pc}}\right), \end{aligned} \tag{35}$$

$$\begin{aligned}\cos(\theta_{v_p',v_p}) &= \hat{\mathbf{v}}_p' \cdot \hat{\mathbf{v}}_P \\ &= \sqrt{\frac{E_p}{E_0 - E_2}} + \frac{E_1}{2\sqrt{E_p(E_0 - E_1)}} (1 - 1/\mu_{pc}). \end{aligned} \tag{36}$$

Here $v_1'$ and $v_2$ are the (intermediate) velocities of the active electrons. From these relations it is clear that heavier projectiles are scattered basically into the forward direction [for $E_0 \gg E_2 \ll E_p', E_0 \approx E_p'$ one obtains $\cos(\theta_{k_0,v_p'}) \approx 1$]. We remark that since $v_1 = v_p$ we obtain $\mu_{pc} k_1 = k_p$ and thus $\mu_{pc} E_1 = E_p$. Equation (35) reduces then to $\cos(\theta_{k_1',v_p}) = (1 - 1/\mu_{pc})/2$. Thus, we obtain for the mutual angle $\theta_{k_1',v_p} \approx 60°$ (in contrast to a positron as a projectile in which case $\theta_{k_1',v_p} = 90° = \theta_{k_2,v_p'}$).

The left-right asymmetry (with respect to $\mathbf{v}_p'$) in the two-particle collision that leads to the ejection of electron 1 [cf. Fig. 2(a)] will result in two *different* structures in the spectrum corresponding to the same perturbation operator [depicted in Figs. 2(a)and 2(a′)]. These two peaks appear [cf. Figs. 2(a) and 2(a′)] at

$$\theta_{k_0,v_p} = \theta_{k_0,v_p'} \pm \theta_{v_p',v_p}. \tag{37}$$

Here the positive (negative) sign corresponds to Fig. 2(a) [Fig. 2(a′)].

In Figs. 2(b) and 2(b′) we investigate yet another variation of the double scattering in which the electron to be captured undergoes at first a scattering from the projectile followed by a collision with the ionic core. The projectile collides then with the second electron ejecting it into the continuum. Consideration of the kinematical conditions and the dichroic effect of the two-body scattering proceeds along the same lines as discussed for the case of Figs. 2(a) and 2(a′).

In the perturbation operators shown in Figs. 2(a)–2(b′) the Green operator of the atom appears. This opens the possibility of a scattering of the ionized electron in the field of the atom. We pointed out in the preceding section that this effect leads to the appearance of the so-called recoil peak. The same happens in the present situation as well. Figures 2 (a″) and 2(a‴) and Figs. 2(b″) and 2(b‴) illustrate the recoil processes corresponding, respectively, to the situations depicted in Figs. 2(a) and 2(a′) and Figs. 2(b) and 2(b′).

The kinematical conditions for the recoil processes are readily obtained from Eqs. (33)–(37) where the angle $\overline{\theta}_{k_0,k_2}$ of the recoil (secondary) electron becomes $\overline{\theta}_{k_0,k_2} = \pi + \theta_{k_0,k_2}$. For a heavy projectile the angle is *fixed* at $\theta_{k_0,k_2} \approx v_2/(2v_0)$ ($v_0$ is the velocity of the incoming projectile). E.g., for $v_2 = v_0$ we expect the recoil peak to be localized at $\overline{\theta}_{k_0,k_2} \approx 240° = -120°$. For simplicity we assume in what follows that $v_0 \gg v_2$ (and therefore $v_p = v_1 \gg v_2$). In this case we deduce from Fig. 2(a″) that the recoil ion momentum is $\mathbf{k}_{\rm ion} = \mathbf{k}_1' - \mathbf{k}_1$ where $k_1' = k_1$. Thus, the ion moves at a *fixed* angle $\theta_{k_0,k_{\rm ion}} \approx 120°$ with respect to the incident direction (note the projectile is scattered predominantly into the forward direction). We can summarize this finding pictorially in Fig. 2(c): When the fully resolved spectrum (spin is not considered here) is scanned as a function of $\theta_{k_0,k_{\rm ion}}$, $\theta_{k_0,k_p}$, and $\theta_{k_0,k_2}$ we expect a peak in the form of a triple ''star,'' as depicted in Fig. 2(c).

The claim is now: the triple *star is two dimensional*. To substantiate this we remark that our mechanisms consist of successive binary encounters each of which takes place in one (scattering) plane. For example, in Fig. 2(a) $\mathbf{k}_0$, $\mathbf{v}_p'$, and $\mathbf{k}_2$ are linearly dependent and lie in one common plane $\mathcal{M}$. From the subsequent binary encounter of the projectile with the electron 1 we conclude that $\mathbf{v}_p'$, $\mathbf{k}_1'$, and $\mathbf{k}_p$ are in the same plane $\mathcal{M}'$. Similarly we conclude that $\mathbf{k}_1'$, $\mathbf{k}_{\rm ion}$, and $\mathbf{k}_1$ are in one plane $\mathcal{M}''$.

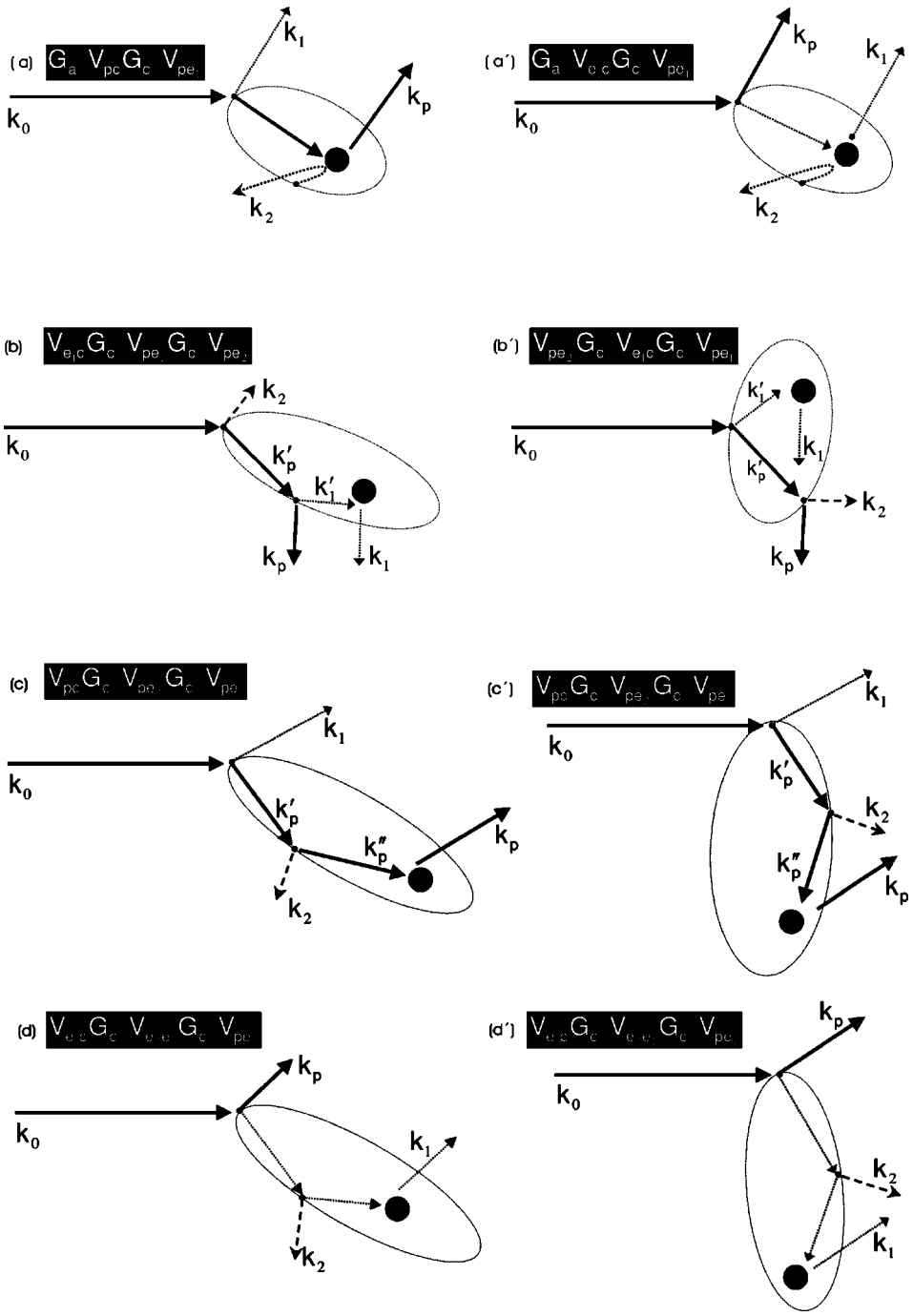


FIG. 3. A graphical representation of the sequential binary collisions contributing to the ionization-transfer–ionization channel when a positron beam is used to induce the reaction. $\mathbf{k}_0$ and $\mathbf{k}_p$ are for the momenta of, respectively, the positron and the positronium whereas $\mathbf{k}_1$ is the momentum of the ionized electron.

We note that $\mathbf{k}_p, \mathbf{k}_1'$ lie in the plane $\mathcal{M}'$ *and* $\mathbf{k}_1', \mathbf{k}_1$ are in the plane $\mathcal{M}''$. Since $\mathbf{k}_1 \| \mathbf{k}_p$ we deduce that $\mathbf{k}_1$ is contained in $\mathcal{M}'$ and therefore $\mathbf{k}_{\rm ion} = \mathbf{k}_1' - \mathbf{k}_1$ must be in $\mathcal{M}'$. In other words, $\mathcal{M}' \equiv \mathcal{M}''$. In addition, Eq. (1) imposes the condition $\mathbf{k}_0/\mu_{pc} - \mathbf{k}_2/\mu_{pc} = \mathbf{v}_p(1+1/\mu_{pc}) + \mathbf{k}_{\rm ion}/\mu_{pc}$. This means if $\mathbf{v}_p$ is fixed by the measurement process to the plane $\mathcal{M}$ the momentum $\mathbf{k}_{\rm ion}$ has no choice but to lie in $\mathcal{M}$ and hence the star is two dimensional and lies in the plane $\mathcal{M}$ (spanned by $\hat{\mathbf{k}}_0$ and $\hat{\mathbf{k}}_2$).

It should be emphasized that the dichroic effect in the two-body scattering as discussed above results in a different spectrum, depending on whether the projectile is scattered to the left or to the right of the incoming beam [cf. Figs. 2(a″) and 2(a‴)].

Further important mechanisms for the ionization-transfer–ionization channel are shown in Fig. 3 and will be analyzed in detail for the positron-impact case. The scattering routes depicted in Fig. 3 are also relevant for the situation of heavy-particle collisions. The analysis proceeds along the same lines sketched below.

### B. Ionization and positronium formation

In the preceding section we discussed double-ionization events in which one of the active electrons is captured by the

projectile. Particular emphasis was put on the case of heavy projectiles. In this section we consider the case of the positron impact. This is of a special interest as the equal masses of the positron and the electrons impose a particular kinematical constraint on the phase space available for the two-body scattering. This is illustrated by the examples shown in Figs. 3(a)–3(d′). In Fig. 3(a) the positron knocks out the first active electron 1 by means of a single (potential) scattering and loses half of its kinetic energy. The second active electron is ejected by virtue of initial-state binding $G_a$ and emerges with much less kinetic energy than the positron (and the first electron). The kinematical conditions under which this process is expected to influence the spectra are $\cos(\theta_{k_1,k_0}) := \hat{\mathbf{k}}_1 \cdot \hat{\mathbf{k}}_0 = \cos \pi/4 = \hat{\mathbf{k}}_p \cdot \hat{\mathbf{k}}_0 =: \cos(\theta_{k_p,k_0})$. The situation depicted in Fig. 3(a′) differs from Fig. 3(a) in that the projectile is scattered only once whereas the first excited electron collides (elastically) with the ionic core to emerge in the same direction as the positron. The kinematical conditions for the processes Fig. 3(a′) and Fig. 3(a) are exactly the same. Hence, it is not possible to distinguish experimentally between them and therefore interference effects might occur when zooming into the particular kinematical situation of Fig. 3(a).

Figure 3(b) illustrates the case where the projectile collides from electron 2 and then from electron 1. The latter scatters then from the ionic core to emerge with the same velocity vector as the positron. The kinematics for this case is specified as $\theta_{k_2,k_0} := \cos^{-1}(\hat{\mathbf{k}}_2 \cdot \hat{\mathbf{k}}_0)$ which is measured by the experiment. Further $\theta_{k_p',k_0} := \cos^{-1}(\hat{\mathbf{k}}_p' \cdot \hat{\mathbf{k}}_0) = \pi/2 + \theta_{k_2,k_0}$ and $\theta_{k_p,k_0} := \cos^{-1}(\hat{\mathbf{k}}_p \cdot \hat{\mathbf{k}}_0) = \theta_{k_p',k_0} + \pi/4$. Here the angles are measured with respect to $\hat{\mathbf{k}}_0$ from 0 to $2\pi$ anticlockwise. The momentum of the recoil ion is then given by $\mathbf{k}_{\rm ion} = \mathbf{k}_1' - \mathbf{k}_1$ where $k_1' = k_1$ and $\cos^{-1}(\hat{\mathbf{k}}_1' \cdot \hat{\mathbf{k}}_0) = \theta_{k_p',k_0} - \pi/4$.

In Fig. 3(b′) there is another constellation in which the projectile undergoes a single scattering on its way out to the continuum from the first and the second electron. The first electron (to be captured) recoils from the ionic core to escape with the same velocity vector as the positron in the final state. From Fig. 3(b′) it is readily deduced that $\mathbf{k}_{\rm ion} = \mathbf{k}_1' - \mathbf{k}_1$ where $k_1' = k_1$. Furthermore,

$$\cos^{-1}(\hat{\mathbf{k}}_1' \cdot \hat{\mathbf{k}}_0) = \cos^{-1}(\sqrt{E_1/E_0}), \tag{38}$$

$$\theta_{k_p',k_0} = \cos^{-1}(\hat{\mathbf{k}}_p' \cdot \hat{\mathbf{k}}_0) = \cos^{-1}(\sqrt{(E_0 - E_1)/E_0}),$$

$$\theta_{k_p,k_0} = \cos^{-1}(\hat{\mathbf{k}}_p \cdot \hat{\mathbf{k}}_0) = \cos^{-1}[\sqrt{(E_0 - E_1)/E_0}] \pm \cos^{-1}[\sqrt{E_p/(E_p + E_2)}], \tag{39}$$

$$\theta_{k_2,k_0} = \cos^{-1}(\hat{\mathbf{k}}_2 \cdot \hat{\mathbf{k}}_0) = \cos^{-1}[\sqrt{(E_0 - E_1)/E_0}] \mp \cos^{-1}[\sqrt{E_2/(E_p + E_2)}]. \tag{40}$$

The positive and the negative signs in, respectively, Eqs. (39) and (40) refer to the situations shown in Fig. 3(b′). The previous discussion of Fig. 2(b) has lead us to the conclusion that the dichroic image shown in Fig. 2(b′) is experimentally distinguishable from Fig. 2(b). Exactly in the same manner as done in Figs. 2(b′) a dichroic process of Fig. 3(b′) can be constructed with the kinematical conditions for its appearance being those as for Fig. 3(b′) [Eqs. (38)–(40)]; however, the negative (positive) sign in Eq. (39) [Eq. (40)] is used.

The four sequential binary collision processes sketched in Figs. 3(c–d′) demonstrate the appearance of dichroic and interference effects for light projectile impact. In Figs. 3(c,c′) the projectile scatters from both active electrons before it collides with the ionic core. The difference between the processes shown in Fig. 3(c) and Fig. 3(c′) is due to the left-right asymmetry (around the momentum direction $\hat{\mathbf{k}}_p'$) in the first positron-electron binary encounter. The kinematical conditions associated with the processes of Figs. 3(c) and 3(c′) are $\theta_{k_1,k_0} = \cos^{-1}\sqrt{E_1/E_0}$ and $\theta_{k_2,k_0} = \cos^{-1}\sqrt{(E_0 - E_1)/E_0} \pm \cos^{-1}\sqrt{E_2/(E_0 - E_1)}$ where the positive (negative) sign corresponds to Fig. 3(c) [Fig. 3(c′)].

From Figs. 3(c)–3(d′) it is clear that Figs. 3(c) and 3(d) correspond to two different terms in the multiple-scattering expansion whose effects appear at the same kinematical situation. Therefore one can expect interference effects between the scattering amplitudes of these two processes. The same applies to the cases depicted in Fig. 3(c′) and 3(d′). It should be emphasized that these interference possibilities occur only when the mass of the projectile is equal to the mass of the electron.

## V. GENERAL AND CONCLUDING REMARKS

In this study we discussed the double electronic transitions in atomic systems induced by charged-particle impact. From an expansion of the four-body scattering operator we identified and explained the physical meaning of the leading-order terms as multiple, sequential binary encounters between the constituent particles of the system. From Eqs. (23)–(32) it is clear, however, that a numerical evaluation of all these facets of the double-excitation reaction within a single (approximate) model is extremely demanding. Most of the theories on the market are therefore restricted to the first Born terms (FBA) in the projectile-target interaction, i.e., in Eq. (6) one neglects the interaction of the projectile of the ionic core *and* in Eq. (5) the interaction of the projectile with all the other particles is omitted. In other words, the projectile performs a free motion in the initial and the final state. Nonetheless, a wealth of ionization mechanisms is still being incorporated in such a model, namely all those that do not involve the scattering of the projectile from the ionic core and from the two electrons in the *final* state. Obviously, the actual weight of the individual (finite) amplitudes might still be inaccurately predicted by the FBA as the evaluation of $G_a$ is a challenging task and can only be done to a certain accuracy.

On the other hand, the FBA treatment, which is usually justified by an appropriate choice of the scattering kinemat-

ics, has the advantage of relating optical spectra to the charged-particle impact spectra. In addition, in a previous work [30] I derived a scaling formula that connects the FBA cross sections for light projectiles with those for heavier ones. Thus the FBA calculation of the spectra for heavy-ion impact is redundant once the FBA results for electron impact are known. In fact it would be of interest to use this scaling recipe to compare the *experimental* data for heavy and light projectiles in the validity range of the FBA. Deviations from the scaling law are then an experimental indication of the importance of higher-order terms in the perturbation expansion.

In this work we unraveled the existence of a dichroic effect in the two-particle collision, i.e., a left-right asymmetry with respect to the incoming beam. This dichroism appears because the two-body scattering is embedded in the four-body background, i.e., the existence of another particle (not participating in the two-body collision) breaks the isotropy of space. This effect is of a general nature and should appear in higher dimensional problems as well.

This dichroic effect also appears in the ionization-transfer–ionization (ITI) channel, i.e., when one of the excited electrons is captured by the Coulomb field of the scattered projectile, as discussed in Fig. 2. We analyzed the multiple-scattering paths in the ITI channel for the case of a heavy projectile (with respect to the electron mass) and for the positron-impact case. For the heavy projectile case we pointed out the appearance of a triple star-form peak in the spectrum when considered as a function of the vector momenta of the ionized electron, the projectile, and the recoiling ion. The existence of this star is induced by sequential two-particle collisions. Superimposed on that is the contributions of the scattering of the continuum electron from the ionic core. This scattering can, in principle, be mediated by $G_a$. As concluded in the text, the two dimensionality of the star is the result of its origin being a sequence of *two*-body encounters. It should be stressed here that the arguments we used to prove that the star is planar are valid generally, i.e., if a continuum multiparticle state is achieved via a sequence of two-particle, isolated collisions we can assume each of the two-particle collisions to be confined to one plane and then consider the angles between the various (two-body) scattering planes to arrive at the final multiparticle configuration.

In the last part of this study we considered the ITI channel when a positron is employed as a projectile. The equal mass of the electrons and the positron caused some of the terms in the multiple-scattering expansion to coincide at the positions where they are expected to appear in the spectrum. Thus we pointed out that interference effects between the scattering amplitudes may occur.

The following final notes are important: (a) the mechanisms discussed in the ITI channel for light- and heavy-particle impact are present is the double-ionization channel (by heavy-ion impact and electron or positron impact) and their kinematical positions are deduced along the same lines as done in the ITI channel. (b) In this work we discussed only a few terms of the expansion (23)–(32). Other terms as well as higher-order terms may affect the spectrum as well. (c) The merit of the present work is to extract and analyze the most important pathways of double excitation. We do not claim, however, that the system will indeed follow a certain pathway just because we pointed out its existence. In other words, only reliable numerical calculations can indicate whether a particular pathway is eventually contributing significantly to the spectrum. (d) The expansion (23) and (32) remain valid at lower energies; however, the kinematical positions we derived for the appearance of the multiple-scattering terms in which $G_a$ is not involved imply high momenta of the particles so that the initial momentum components contained in $G_a$ become irrelevant. (e) The expansion (23)–(32) has been derived using operator algebra and as such is generally valid. However, if the matrix elements are to be calculated, i.e., when expressing (23)–(32) in a certain representation, one encounters serious convergence problems due to the infinite range of the Coulomb potentials. To circumvent this problem one either introduces a cutoff parameter for the potential or calculates the matrix elements off the energy shell. The on-shell limit is then performed in the final expression.

## ACKNOWLEDGMENT

I am indebted to Horst Schmidt-Böcking for stimulating discussions and for his continuing encouragement to consider the ITI process.

[1] V. Mergel, R. Dörner, M. Achler, Kh. Khayyat, S. Lencinas, J. Euler, O. Jagutzki, S. Nuttgens, M. Unverzagt, L. Spielberger, W. Wu, R. Ali, J. Ullrich, H. Cederquists, A. Salin, C.J. Wood, R.E. Olson, D. Belkic, C.L. Cocke, and H. Schmidt-Böcking, Phys. Rev. Lett. **79**, 387 (1997).

[2] R. Wehlitz, M.-T. Huang, B.D. DePaola, J.C. Levin, I.A. Sellin, T. Nagata, J.W. Cooper, and Y. Azuma, Phys. Rev. Lett. **81**, 1813 (1998).

[3] I. Taouil, A. Lahmam-Bennani, A. Duguet, and L. Avaldi, Phys. Rev. Lett. **81**, 4600 (1998).

[4] A. Dorn, R. Moshammer, C.D. Schröter, T.J.M. Zouros, W. Schmitt, H. Kollmus, R. Mann, and J. Ullrich, Phys. Rev. Lett. **82**, 2496 (1999).

[5] M. Unverzagt, R. Moshammer, W. Schmitt, R.E. Olson, P. Jardin, V. Mergel, J. Ullrich, and H. Schmidt-Böcking, Phys. Rev. Lett. **76**, 1043 (1996).

[6] B. El-Marji, J.P. Doering, J.H. Moore, and M.A. Coplan, Phys. Rev. Lett. **83**, 1574 (1999).

[7] R. Moshammer, J. Ullrich, H. Kollmus, W. Schmitt, M. Unverzagt, O. Jagutzki, V. Mergel, H. Schmidt-Böcking, R. Mann, C.J. Woods, and R.E. Olson, Phys. Rev. Lett. **77**, 1242 (1996).

[8] A. Lahmam-Bennani *et al.*, Phys. Rev. A **59**, 3548 (1999).

[9] B. Bapat, S. Keller, R. Moshhammer, R. Mann, and J. Ullrich, J. Phys. B **33**, 1437 (1999).

[10] C. Dal Cappello and H. Le Rouzo, Phys. Rev. A **43**, 1395 (1991).

[11] J. Berakdar and H. Klar, J. Phys. B **26**, 4219 (1993).

[12] A. Kheifets *et al.*, J. Phys. B **32**, 5047 (1999).
[13] D. Belkic, I. Mancev, and V. Mergel, Phys. Rev. A **55**, 378 (1997).
[14] R. El Mkhanter and C. Dal Cappello, J. Phys. B **31**, 301 (1998).
[15] A.W. Malcherek, J.-M. Rost, and J.S. Briggs, Phys. Rev. A **55**, R3979 (1997).
[16] T. Ishihara and J.H. McGuire, Phys. Rev. A **38**, 3310 (1988); J.H. McGuire *et al.*, Phys. Rev. Lett. **62**, 2933 (1989).
[17] L.H. Thomas, Proc. R. Soc. London, Ser. A **114**, 561 (1927).
[18] K. Dettmann and G. Leibfried, Z. Phys. D: At., Mol. Clusters **218**, 1 (1969).
[19] R. Shakschaft and J.M. Wadehra, Phys. Rev. A **22**, 968 (1980).
[20] R. Shakeshaft and L. Spruch, Phys. Rev. Lett. **41**, 1037 (1978).
[21] E. Hordsal-Pedersen, L.C. Cocke, and M. Stöckli, Phys. Rev. Lett. **50**, 1910 (1983).
[22] R. Shakeshaft and L. Spruch, J. Phys. B **11**, L457 (1978).
[23] J.S. Briggs, J. Phys. B **19**, 703 (1986).
[24] J.S. Briggs, Comments At. Mol. Phys. **23**, 155 (1989).
[25] M. Brauner and J.S. Briggs, J. Phys. B **24**, 2227 (1991).
[26] J. Berakdar and H. Klar, J. Phys. B **26**, 3891 (1993).
[27] J. Palinkas, R. Schuch, H. Cederquist, and O. Gustafsson, Phys. Rev. Lett. **63**, 2464 (1989).
[28] E. Hordsal, B. Jensen, and K.O. Nielsen, Phys. Rev. Lett. **57**, 1414 (1986).
[29] H. Ehrhardt, K. Jung, G. Knoth, and P. Schlemmer, Z. Phys. D: At., Mol. Clusters **1**, 3 (1986).
[30] J. Berakdar, J. Phys. IV **3**, C6-135 (1993).